Research Article

Quartz crystal microbalance as cell-based biosensor to detect and study cytoskeletal alterations and dynamics[†]

Monica Bianco[1]
Daniele Vergara[2,3]
Stefania De Domenico[4,5]
Michele Maffia[2,3]
Antonio Gaballo[1]
Valentina Arima[1]

[1]CNR-NANOTEC, Institute of Nanotechnology c/o Campus Ecotekne, Lecce, Italy

[2]Department of Biological and Environmental Sciences and Technologies, University of Salento, Lecce, Italy

[3]Laboratory of Clinical Proteomics, ''Giovanni Paolo II'' Hospital, ASL-Lecce, Italy

[4]Biotecgen, c/o Department of Biological and Environmental Sciences and Technologies, Lecce, Italy

[5]Institute of Sciences of Food Production, National Research Council, Lecce, Italy

Correspondence: Monica Bianco, CNR-NANOTEC, Institute of Nanotechnology c/o Campus Ecotekne, University of Salento, Via per Arnesano, 73100 Lecce, Italy.

E-mail: monica.bianco@nanotec.cnr.it

Correspondence: Antonio Gaballo, CNR-NANOTEC, Institute of Nanotechnology c/o Campus Ecotekne, University of Salento, Via per Arnesano, 73100 Lecce, Italy.

E-mail: antonio.gaballo@nanotec.cnr.it

Keywords: Actin, Cytoskeleton, Quartz crystal microbalance, Y27632

Abbreviations: CytoD, cytochalasin D; **FAK**, Focal adhesion kinase; **QCM-D,** Quartz Crystal Microbalance with Dissipation Monitoring; **ROCK,** Rho kinase.

[†]This article has been accepted for publication and undergone full peer review but has not been through the copyediting, typesetting, pagination and proofreading process, which may lead to differences between this version and the Version of Record. Please cite this article as doi: [10.1002/biot.201700699].

Received: November 15, 2017 / Revised: March 9, 2018 / Accepted: March 23, 2018

Abstract

Several techniques can be used to monitor cell dynamism after a perturbation. Among these, Quartz Crystal Microbalance with Dissipation Monitoring (QCM-D) offers the great advantage to study the mechanical properties of cells in real-time and with a great sensitivity. Here, we used QCM-D to investigate the effects of two cytoskeleton-targeting agents, cytochalasin D (CytoD) and Y27632, on human MCF-7 cells. Cell adhesion on the sensor surface, crucial for in-flow experiments, was obtained by covalent adsorption of a fibronectin (FN) film, an extracellular matrix (ECM) protein. Direct analysis of MCF-7 cells on FN-coated sensor, showed a specific cellular response that was revealed and quantified by QCM-D after drugs exposure. Notably, upon treatment with Y27632, we observed a two-regime dissipation behaviour that we associated with specific modifications of actin filaments and signaling proteins providing a link between biophysical and molecular mechanisms. Overall, this approach opens new opportunities for studying cellular response to mechanical cues in different biological conditions.

1 Introduction

Dynamic cytoskeleton modifications, in response to either extracellular or intracellular events, are responsible for altering the mechanical phenotype of the cells and thus the function of multiple molecular and biochemical pathways. These include changes in cellular processes that characterise both physiological and pathological conditions and that impact on cell assembly and morphogenesis, motility, and mitosis. Alterations in the expression and localization of cytoskeletal proteins contribute to the onset and progression of various pathologies and diseases including cancer and neurodegenerative disorders [1, 2]. For example, breast cancer cell models modify the expression of cytoskeletal proteins during the process of epithelial-mesenchymal transition (EMT), with a significant impact on cell organization and motility [1]. In consideration of this, cellular cytoskeleton is the main target of different therapies and intervention strategies. This includes classical chemotherapeutic agents (such as Paclitaxel), as well as chemical inhibitors directed towards main cytoskeletal regulators. Among these, Rho kinase (ROCK) inhibitors represent a class of molecules with a broad range of applications from hypertension to cancer [3].

Recently, biosensors are emerging as innovative and highly sensitive methods to acquire time-course data of processes occurring at the sensor interface [4]. The dynamic nature of cytoskeleton morphologic changes can be readily analysed using label-free biosensors to reveal time-resolved information. Specifically, Quartz Crystal Microbalance with Dissipation Monitoring (QCM-D) is a non-invasive and acoustic sensing system capable of real-time monitoring of the interaction between cells and the surface of the sensing element [5]. QCM-D detects changes in resonance frequency and dissipation of a quartz crystal oscillated by a shear wave resonator with high sensitivity and low noise [6, 7]. Over the past two decades such a unique capability has made the QCM-D particularly attractive in the field of cell biology [8-15] for its capability to study cells in a label-free manner [12, 13, 16-18], to determine the kinetics of cell attachment and spreading [19, 20] and monitor the long term growth of cells [21, 22] as well as cell viscoelasticity [23-28]. On the micro-scale sensor cells can be seeded and treated with different stimuli for monitoring temporal variations of their biophysical properties.

This represents a major advantage of QCM-D over classical biological approaches that require fixation steps and post-treatment analysis procedures. Even samples in suspension can be tested, by monitoring the adhesion of a cell to a particular substrate.

In this study, the cytoskeleton alterations induced by the ROCK inhibitor Y27632 are directly analysed using a QCM-D system in the epithelial breast cancer cell line model MCF-7, and compared to the changes induced by CytoD treatment, a widely used inhibitor of actin dynamics. This experimental approach offers several advantages compared to classical optical/confocal microscopy techniques that are limited by experimental errors due to sample-light interactions or erroneous optical beam path inside the microscope and provide end-point measurements, which result more time-consuming and laborious for monitoring on-going modifications [29]. Although CytoD was widely used in the QCM study of various cells [7, 30], Y27632 was studied for the first time by QCM-D in this work.

QCM-D analysis of MCF-7 treated with Y27632 revealed a distinct and time-dependent dissipation profile if compared to CytoD, which was correlated to different structural and mechanical properties of the adhered cells in response to drug stimuli. By complementary techniques, we demonstrated that these signals were the results of specific actin cytoskeletal modifications, affecting cell shape and organization. As investigated by western blotting analysis, this reflects more specific molecular alterations induced after Y27632 treatment that acts by regulating the expression of actin-binding proteins. In this way, we provide a functional link among the QCM-D dissipation signals, actin network organization, and molecular mechanical properties.

Overall, these results open new possibilities for the implementation of QCM-D for the analysis of novel pharmaceutical formulations targeting cytoskeleton.

2 Materials and methods

2.1 Chemicals

Phosphate Buffer Saline solution (PBS, pH 7.4 Dulbecco A., Axoid), Mercaptoundecanoic acid (MUA), N-(3-Dimethylaminopropyl)-N-ethylcarbodiimide hydro-chloride (EDC), and N-hydroxysuccimide (98%) (NHS) were purchased from Sigma Aldrich (Milan, Italy). Absolute ethanol and acetone were

purchased from Carlo Erba (Italy). Fibronectin (FN), Dulbecco's Modified Eagle Medium high glucose (DMEM), (3-Aminopropyl)triethoxysilane (APTES), 2.5% Glutaraldehyde, L-glutamine, fetal bovine serum (FBS), penicillin and streptomycin, Phalloidin–Tetramethylrhodamine B isothiocyanate (TRITC), and Fluoroshield were purchased from Sigma Aldrich (Milan, Italy). Leibovitz's L-15 medium, Cytocalasin-D (CytoD) and Y27632 were from Tocris. Ultrapure water with a resistivity of 18.2 M was used (Purelab). Ammonium hydroxide (28–30%), sulfuric acid (H_2SO_4, 30%) and hydrogen peroxide, H_2O_2, (30%) were purchased from Baker. Blotto A, primary and secondary antibodies were from Santa Cruz Biotechnology: E-cadherin (sc-8426), β-catenin (sc-7963), γ-catenin (sc-514115), Vinculin (sc-73614), Cofilin (sc-33779), phospho-Cofilin (ser3) (sc-21867-R), mouse anti-goat IgG-HRP (sc-2354), goat anti-rabbit IgG-HRP (sc-2004), β-Actin (#8457), Focal adhesion kinase (FAK) (#3285), and phospho-FAK (tyr397) (#3283). Myosin light chain 2 (MLC) (#3672), phospho-Myosin light chain 2 (ser19) (#3671) and RIPA extraction buffer were from Cell Signaling Technology.

2.2 Cell culture

Human tumor cells were purchased from Banca Biologica and Cell Factory (IRCCS Azienda Ospedaliera Universitaria San Martino-IST Istituto Nazionale per la ricerca sul cancro, Genova, Italy). The human cancer cell line MCF-7 was cultured in high glucose DMEM (Sigma Aldrich) supplemented with 10% FBS (Sigma Aldrich), 100 U/mL penicillin and 100 μg/mL streptomycin at 37° C in an atmosphere of 5% CO_2.

2.3 Bright-phase microscopy analysis

To study morphological effects of CytoD on MCF-7 cells on different substrates, bright-phase microscopy images were obtained using an Olympus IX51 microscope (10x magnification). For every treatment, four random fields of vision were acquired. Three samples were prepared named "uncoated", "chemFN" and "physFN". On the uncoated sample, MCF-7 cells were seeded on glass coverslips in absence of FN and treated with 10 μM CytoD for 15 and 40 min. The same procedure was repeated on glass coverslips incubated for 2h at 37°C with 10 μg/mL of sterile FN solution (physFN)

and on glass coverslips functionalized by using the silane chemistry [31] (chemFN). In the case of chemFN, the glass coverslips, after cleaning by H_2O_2:H_2SO_4 solution 1:3 and washing with water, were incubated in 10% APTES in ethanol for 3h. After washing with ethanol, the samples were incubated for 1 h in 2.5% Glutaraldehyde. After washing, FN was deposited as reported for physFN followed by washing with sterile PBS.

2.4 Confocal immunofluorescence microscopy analysis

For confocal microscopy analysis, $3x10^4$ MCF-7 cells were grown onto glass coverslips coated with 10 μg/mL of sterile FN solution (nonspecific physical adsorption) that was directly added to coverslips and incubated for 2h at 37°C. The day after, cells were treated with 10 μM CytoD or with 10 μM Y27632 for 5, 15 and 40 min. Control cells were treated with the vehicle used to dissolve CytoD and Y27632 (DMSO, 0.01% v/v).

Before microscopy analysis, cells were washed three times with PBS buffer, fixed for 10 min in 4% paraformaldehyde and washed three times by PBS buffer prior to staining.

For F-actin staining, seeded cells were fixed and permeabilized with ice cold acetone for 15 min. Fixed cells were washed twice with ice cold PBS and incubated with TRITC according to the manufacturer's protocol. Slides were cover-slipped using a mounting medium (Fluoroshield) containing 4′ 6-diamidino-2-phenylindole (DAPI) in order to counterstain nuclei.

The images of fluorescently labelled proteins were captured using a confocal laser scanning microscope (CLSM) (TCS SP5; Leica, Microsystem GmbH, Mannheim, Germany) equipped with a laser diode emitting at 405 nm, an argon-ion laser for excitation at 488 nm (50%), and a helium-neon laser for excitation at 514 nm (50%). The fluorescence signal of DAPI (blue channel) was detected after filtering with a band pass filter within the range 415-500 nm and TRITC-phalloidin (red channel) was detected with a 565-660 nm band pass filter. Images were taken with a HCX PL APO lambda blue 63.0x1.40 oil-immersion objective under sequential mode acquisition (scan mode: xyz; scan speed: 200 Hz). The pinhole aperture was set to 1 Airy.

2.5 Western blotting

Western blotting was performed as previously described with minor modifications [1]. In detail, cells seeded on FN-coated (10μg/mL, nonspecific physical adsorption) and uncoated dishes in the exponential growth phase were lysed in RIPA extraction buffer, proteins resolved in 12 % sodium dodecyl sulfate-polyacrylamide gel (SDS-PAGE) and transferred to nitrocellulose membrane (GE Healthcare, Little Chalfont, UK). After incubation with 5% nonfat milk and 0.05% Tween-20 (Blotto A) for 1 h, blots were probed with specific primary antibodies for 1 h at room temperature. Membranes were washed two times for 10 min with a TBST solution (10 mM Tris, pH 8.0, 150 mM NaCl, 0.5% Tween 20) and incubated with a 1:2000 dilution of horseradish peroxidase-conjugated secondary antibodies for 2 h at room temperature. Membranes were washed two times with TBST and detected using the Amersham ECL western blotting detection system according to the manufacturer's protocols (GE Healthcare, Little Chalfont, UK). Bright-phase images of the dishes were obtained using an Olympus IX51 microscope.

2.6 Preparation of FN/MCF-7 coated sensors

Before each experiment, QCM-D sensors were placed in a plasma cleaner (Pico, Diener Electronic) for 10 min and then cleaned with a heated solution of 1:1:5 ammonium hydroxide, H_2O_2 and ultrapure water; then treated again with oxygen plasma for 1 min and rinsed with ultrapure water and ethanol. The cleaned gold sensor surfaces were functionalized *ex-situ* using the MUA/NHS/EDC procedure [32]. Briefly, the QCM-D sensor was immersed overnight into a 10 mM ethanol solution of MUA in order to obtain the thiol self-assembled monolayer (SAM). After rinsing, the crystal was incubated for 3 h into a mixture of 15 mM NHS and 75 mM EDC for activation of carboxyl groups. After rinsing, the QCM-D sensor was left to soak for 30 min in 10 μg/mL FN solution in sterile PBS under the laminar flow of a biological safety cabinet. The cells were seeded on the sensor into an individual well of a 6-well cell culture plates as follows: the sensor was equilibrated in sterile PBS prior to deposition of 3 mL of sterile and complete DMEM supplemented with 10 % (v/v) heat-inactivated FBS, 1 % (v/v) penicillin, streptomycin and 1 % (v/v) L-glutamine. This medium is called complete medium (CM) in the rest of

the manuscript. After a 30 min incubation at 37°C, the CM was removed and 50,000 or 33,000 cells in 50 μL of CM were deposited on the surface of the sensor. Cells were allowed to attach for 30 min at 37°C under a 5 % CO_2 atmosphere; soon after, 3 mL of CM at 37°C were added to the sensor and incubated overnight at 37°C under 5 % CO_2 atmosphere.

2.7 Preparation of MCF-7 coated sensors

A protocol for sensor functionalization in absence of FN was also developed. After cleaning procedure described at the paragraph 2.6, under a laminar flow biological safety cabinet, the sensor surface was exposed to UV light for 15 min. The QCM-D sensor was placed into an individual well of a 6-well cell culture plate and equilibrated with CM for 1 h at 37°C; then, the CM was removed and 50,000 or 33,000 cells in DMEM (50 μL) were added on the sensor surface. The cells were allowed to attach and grow under humidified atmosphere for 30 min at 37°C and 5 % CO_2; immediately after, 3 mL DMEM at 37°C were added and the sensor placed overnight at 37°C under a 5 % CO_2 atmosphere.

2.8 QCM with dissipation monitoring (QCM-D)

QCM-D measurements were acquired using the E1 Q-Sense system and gold-coated quartz sensors. Similarly to our previous works [33], the resonance frequency was measured simultaneously at the fundamental and at the six harmonics during the interaction steps, but the measurements at natural frequency (5 MHz) were not considered being highly sensitive to bulk solution changes. For simplicity, only changes at the 5^{th} overtone, as the most representative of the set of experiments, were presented in the graphs reported in Fig. 2A,B,D and in Suppl. Fig. 1. The maintaining of a constant temperature (37°C) in the QCM-D chamber was controlled and recorded as a function of time during the entire experiment. All solutions were degassed before injection in the QCM-D chamber.

The QCM-D sensors treated as reported in par. 2.6 and 2.7, were immersed for 1 h at 37°C under a 5 % CO_2 atmosphere in Leibovitz's L-15, a medium suitable for supporting cell growth in environments without CO_2 equilibration. Then the medium was removed and the sensors were placed in the QCM-D chamber after removing the residual buffer from the back-side. After achieving a stable baseline, the

medium was replaced with a 10 μM drug solution dissolved in L-15 medium. Frequency (Δf) and dissipation (ΔD) signals have been detected during drug injection and static incubation for about 1h at 37°C. Two different types of cytoskeleton drugs were used: i) CytoD, that hinders the polymerization of actin in the cytoskeleton and induces dramatic changes in cell morphology, and ii) Y27632 that performs pharmacological inhibition of Rho-associated protein kinase activity [34].

The changes in Δf and ΔD of the sensor surface during the binding experiments were recorded using the Q-Soft software and the data were analyzed using the Q-Tools (Q-Sense, Sweden) and Origin 8 software (OriginLab Corporation, Northampton, MA). All experiments were repeated using a second set of sensors prepared using the same procedure.

3 Results

3.1 QCM-D characterization of MCF-7 cells seeded on FN-coated sensor

In this study, the effect of substrate-protein interaction on MCF-7 cellular behaviour was investigated administering to cells two cytoskeleton-targeting drugs, in presence or absence of fibronectin (FN), an extracellular matrix component that plays a crucial role in adhesion-dependent cellular activities, such as attachment, proliferation, and differentiation [35]. FN deposition on sensor surface is expected to promote cell attachment and spreading. The effect of drugs was tested: CytoD, an F-actin-disrupting drug that has been extensively studied for assessing the role of cytoskeleton, and Y27632, a ROCK inhibitor.

FN has been covalently attached to the QCM gold sensor in order to produce a layer that facilitates cellular binding through integrin receptors [36, 37]. This preparation method is simple, fast, highly reproducible and characterized by a well-defined surface chemistry and a stable chemical immobilization [38]. In particular, FN attachment to the modified gold surface takes place via 1-Ethyl-3-(3-dimethylaminopropyl) carbodiimide (EDC) coupling reaction as described in Fig. 1A. Amide self-assembled monolayer (SAM) refers to surface chemistries involving thiol SAM and probes immobilized via an amide bond. The amide bond was formed between the carboxyl group of the MUA and the amine

groups of the FN to be immobilized; to form the amide bond, the carboxy-ended layer was activated with EDC and NHS (Fig. 1A). The superior suitability of grafted FN compared with physisorbed FN coatings in QCM-D cell studies have been demonstrated by Kandel et al. without relevant effects on cells viability, structure and metabolism [7]. Preliminarily, we verified that the deposition method of FN was not the main determinant of drug action. To this aim, we seeded MCF-7 on classical glass coverslips coated or not with FN chemically (chemFN) or physically adsorbed (physFN). As observed in Suppl. Fig. 2, morphological changes associated with drug treatments are visible in all tested conditions. This means that the effect of cytoskeleton disrupting drugs on MCF-7 is not dependent on the FN assembly.

After production of a FN adhesive layer, cells were seeded on the sensor surface as described in the materials and methods section, and placed into the QCM-D chamber. A reference sensor without FN was also prepared as described.

All the QCM-D signals induced by the cell reaction to the vehicle or to the different drugs treatments were monitored only after achieving a stable baseline for both frequency (Fig. 2C) and dissipation (data not reported) at the fifth harmonics. The L-15 medium was pumped at the lower constant rate of 14 μLm^{-1} using a peristaltic pump for 40 min. Fig. 2C shows that after 30 min stable baselines were established for the measurements described in Fig. 2A,B,D, and all the baselines were re-zeroed prior to the addition of drugs.

At first, we compared the response to CytoD of MCF-7 cells cultured on FN-coated and on uncoated sensors (Fig. 2A,B and Suppl. Fig. 1). While frequency shifts appeared negligible for both samples (Fig. 2A), a characteristic decrease in dissipation was observed in MCF-7 attached on FN-coated sensor and treated with 10 µM CytoD (Fig. 2B and Suppl. Fig. 1). A weak energy dissipation decrease was detected in absence of FN, but it could be confused with experimental variation. This means that the effect of CytoD on MCF7 cells is detectable by QCM only when they are seeded on a FN-coated gold substrate and that the uncoated gold sensor is not suitable because it does not support the physiological adhesion of cells. The reason for that was exploited by analysing protein expression in presence and in absence of FN. We observed (Fig. 1B) that the mechanical interaction between MCF-7 cells and FN

influences protein expression, leading to an increased phosphorylation of FAK and MLC that may influence the formation of integrin-FN adhesion contacts (Fig. 1B). Cell spreading was also promoted after the binding with FN. As shown in Fig. 1C, MCF-7 cells seeded on the FN-coated substrate spread by putting out cellular extensions like filopodia-like projections and lamellipodia. Therefore, the FN-coating offering a more biocompatible substrate is essential to modify the gold sensor in order for cellular response to occur in QCM-D experiments.

3.2 QCM-D detection of the cell response to drugs targeting actin cytoskeleton

Having established that cells have a greater adhesion on FN-coated sensors and that dissipation signal has a higher sensitivity to cytoskeleton-related changes, we proceeded to evaluate the early-stage effects associated to the treatments of MCF-7 with two cytoskeleton-perturbing agents as changes in viscoelastic properties at cells layer-sensor interface.

CytoD and Y27632, were chosen to evaluate the sensitivity of QCM-D to discriminate cells-drug interaction mechanisms [39]. Doses of CytoD that induce a visually-detectable effect are usually in the range 1–10 μM [40], while effective doses of Y27632 are around 10 times higher [40]. In this study, both drugs were used at 10 μM, a concentration that had no significant effect on cell proliferation at any time points (data not shown).

As already observed, the addition of CytoD, a drug that directly depolymerizes the actin filaments of the cytoskeleton, resulted in a negative shift in ΔD. The signal reached its minimum value after 40 min from the beginning of the measure and after 10 min from drug injection, then becoming stable (Fig. 2D). On the other hand, the addition of the ROCK inhibitor Y27632 to the MCF-7 layer, first induced an initial ΔD decrease at about 8-10 min from the addition of the drug, followed by a rapid rise in ΔD at 30 min from the beginning of the experiment (about 20 min from drug injection) with a shift of the dissipation signal towards higher values (Fig. 2D).

3.3 Y27632 regulation of the actin cytoskeleton and of the phosphorylation of actin cytoskeleton-associated proteins

To uncover cellular and molecular determinants of QCM-D measurements, optical and confocal microscopy images were acquired at the same time points for the two drugs studied. To obtain information about the effect of chemotherapy drugs on the organization of actin filaments, QCM-D measures were complemented with phase contrast and CLSM images (Fig. 3B and 4B). For this purpose, MCF-7 cells were seeded onto glass coverslips coated with 10 μg/mL of sterile FN solution and incubated in the presence of 10 μM CytoD or with 10 μM Y27632 for 5, 15 and 40 min, respectively. Control cells (CTR) were treated with vehicle (DMSO). After fixation, cells were fluorescently labelled using TRITC-phalloidin and DAPI to stain the F-actin and nuclei, respectively. Phenotypically, we noticed that treated cells show remarkable morphological changes as compared with CTR cells, that are characterised by a typical cobblestone morphology and dense stress fibers in the central and peripheral portion of the cell. In particular, treatment of MCF-7 with 10 μM CytoD induces the already described morphological changes such as, shrinkage and disruption of the cytoskeletal structure, disappearance of stress fibers, formation of aggregates first at the periphery of the cell and then after 15 min and 40 min progressively throughout the cell. A rounding of the perinuclear area is also evident (Fig. 3A,B). MCF-7 cells treated with 10 μM Y27632 are characterized by a progressive decrease of the actin filaments bundles and marked differences in cell shape (Fig. 4A,B), a result that is functionally correlated to the role that ROCK has in the regulation of actin cytoskeleton and cell-cell adhesion components.

Overall, CytoD has a more severe effect on actin structure compared to Y27632, an effect that is observed after few minutes of treatment. This may induce cytoskeletal modifications that are rapidly detected by QCM and that persist even after 80 min of analysis (Fig. 2). This is in accordance to the morphological analysis of MCF-7 treated with CytoD at 40 min of stimulation that revealed a profound effect on cellular structure (Fig. 3A,B). However, this observation raises the question about the molecular mechanisms that may be responsible for the observed cellular modifications. To investigate this, we studied the expression and localization of proteins involved in the regulation of actin assembly and cell-cell adhesion by western blotting in MCF-7 treated cells (Fig. 3 and Fig. 4). As shown, E-cadherin, β-catenin, Vinculin and γ-catenin did not reveal significant differences in the expression

levels in CytoD and Y27632 treated cells compared to CTR (Fig. 3C and Fig. 4C). On the contrary, the phosphorylation status of cofilin, myosin, and FAK appeared modified. In particular, our findings in cultured MCF-7 show that CytoD reduces significantly myosin and FAK phosphorylation after both 15 min and 40 min of treatment (Fig. 3C). Y27632 has major effects on phospho-cofilin and phospho-myosin, and to a lesser degree on FAK than CytoD treatment (Fig. 4C). This suggests that morphological effects of CytoD and Y27632 may be also related to a different effect on actin remodelling proteins.

4 Discussion

QCM-D is a highly sensitive mechanical sensor able to directly detect changes in resonant oscillation parameters that are caused by viscoelasticity (changes in dissipation ΔD) or mass (changes in frequency Δf) modifications at a piezoelectric crystal interface.

In the present study, QCM-D has been used to make a comparative real-time analysis of cytoskeleton alterations induced on MCF-7 cancer cells, grown in presence or absence of FN, by treatment with two anticancer drugs, the ROCK inhibitor Y27632 and an actin-disrupting agent, CytoD.

The viscoelastic variations detected by QCM-D were then integrated with confocal microscopy and other biochemical analytical techniques, to correlate the cellular nanomechanical layout to the underlying specific molecular alterations.

The presence of a FN-coated sensor allowed to growth cells in a more physiological state by improving cell-substrate adherence, generating a biochemical signal that led to the activation of myosin and FAK, as demonstrated by western blot analysis (Fig 1B). This also improved QCM-D analysis (Fig. 2A,B and Supp. Fig. 1). The weak frequency shift detected in Fig. 2A for both samples means that no cell detachment occurs during the 1h treatment with CytoD as confirmed by the optical inspection (Fig. 3A). However, the weak fluctuation of the frequency signal for the sample without FN maybe correlated to some instabilities of the cell monolayer during drug treatment.

Treatment with CytoD of MCF-7 cells seeded on FN results in a rapid cell stiffening as shown by a dramatic dissipation signal shown in Fig. 2B. On the other hand, a very weak dissipation signal was

recorded for FN-uncoated sample (Fig. 2B and Supp. Fig. 1). To better explain this different cyto-mechanical behaviour the biological role of FN in the adhesion and spreading of breast cancer cells has to be considered. Teng's research group [41] investigated the effects of FN on the biological and biomechanical characteristics of MCF-7 cells performing adhesion, spreading, proliferation, migration, and elasticity assays. Authors demonstrated that mechanical and cellular behaviors are inextricably associated, and influenced by the binding with ECM components. For example, MCF-7 cells became significantly softer when grown on FN matrix [42]. Moreover, the adhesion on FN stimulates the phenomena of mechanotransduction that involves the activation of protein kinases, as we demonstrated in Fig. 1B. Therefore, the more intense dissipation signal and the more stable frequency during the CytoD treatment for the FN/MCF-7 sample are both due to the major role played by FN in promoting and keeping cell adhesion to the sensor surface which in turn results in an increased QCM-D sensitivity to the cell-substrate binding events.

The versatility of QCM-D in combination with a multitude of surface chemically modified sensors provides a useful system for making comparisons among cell types. One area of future work will be the immobilization of other ECM proteins (i.e. collagen, elastin, laminin) to study the interaction of cells with different ECM components with practical applications in multiple aspects of cell physiology or therapeutic response.

Here, the mechanisms of drug-induced cytoskeleton disruption were exploited during QCM-D studies shown in Fig. 2D that compare the dissipation signal detected in MCF-7 seeded on FN upon CytoD addition with that measured upon treatment with Y27632. CytoD causes a dramatic decrease of energy dissipation of the cellular layer thus suggesting a drug-induced drastic increase in rigidity. Furthermore the depolymerizing effect of 10 μM CytoD appears to be saturated already after 20 minutes treatment. The intensity of the energy dissipation decrease was of $1.7 * 10^{-6}$ (5th overtone). Tymchenko et al. registered a value of $\approx 4 * 10^{-6}$ (5th overtone) after CytoD addition (2 μg/mL) to 3T3 cells grown on a Collagen I layer physisorbed at the sensor interface [30]. Kandel et al. [7] reported dissipation changes of $\approx 2.2 * 10^{-6}$ (5th overtone) due to CytoD addition (1 μM) to human dermal fibroblasts on chemisorbed FN. The dissipation values we registered are more similar to Kandel's than

to Tymchenko's works, probably because of the use of grafted FN in both studies. However, other factors may be responsible for the observed differences including the cell models used to perform experiments (fibroblast vs epithelial models) which probably organize in a different way at the sensor interface leading to a more intense mechanical response, as well as cell culture conditions including number of seeded cells and treatment.

The dissipation decrease following the CytoD treatment was attributed by Tymchenko et al. to changes in the mechanical interaction between the cell and the protein layer induced by actin mesh alteration [30]. Furthermore, CytoD was reported to act on cell-surface contacts competing against proteins that bind the actin to the sensor surface [43].

The response of QCM to Y27632 and CytoD treatment is different and probably related to their different mechanism of action observed in MCF-7 cells. An accurate reading of the Y27632 spectrum (Fig. 2D) indicates that Y27632 (at a 10 μM concentration) exerts its activity on the MCF-7 cells seeded on FN only after an incubation of 8-10 min from the drug injection. After this time point, cells display a higher stiffness as revealed by a decrease of energy dissipation. This behaviour appears to be completely inverted by a more delayed process that determines an increase of dissipation. This effect persists after more than one hour of treatment.

Thus, treatment with 10μM CytoD resulted, as expected [40], in a drastic and irreversible effect on MCF7 cells. The rigid layer at the QCM sensor-cell interface, detected after CytoD treatment, can be explained by a rapid disruption of actin filaments even after few minutes of drug incubation as demonstrated by the accumulation of actin aggregates visible under CLSM (Fig. 3B). At a molecular level, this effect follows a specific program characterised by a significant decrease of both FAK and myosin phosphorylation (Fig. 3C) that contributed to the final and irreversible loss of contractility. On the other hand, we hypothesize that the two-regime dissipation behaviour observed after Y27632 treatment could be due to the use of a sub-effective Y27632 concentration which could determine a biphasic temporal and mechanical Y27632 effect, by regulating actomyosin complex and FAK. Initially, in a manner similar to what observed for CytoD, Y27632 created a more rigid layer with a negative dissipation value corresponding to a rapid myosin II and cofilin dephosphorylation which lead to the

actin fibers depolymerization and loss of contractility [44]. After 20 min from drug injection, other molecular mechanisms, such as dephosphorylation of FAK, probably become dominant altering organization of focal adhesions mechanical linkages to the external fibronectin. Such configuration, as a consequence, may originate a softer layer with an increase of dissipation value. The softening effect of Y27632 has been reported for different cell lines as H9C2 cardiomyoblasts investigated by high-throughput QCM chips [45] and MDA-MB-231 metastatic breast cancer cells using Atomic Force Microscopy [46]. The dissipation increase is also consistent with a previous confocal microscopy observation for MCF7 transfected cells [47] that described the ability of Y27632 to sever actin filaments in addition to softening it, and by our CLSM experimental findings that demonstrated the disappearance of elastic and compact stress fibers (Fig.4B). We further observed the effects of Y27632 on FAK phosphorylation and a reduction of phospho-FAK after 40 min of treatment (Fig. 4C). This suggests that FAK activity is not immediately affected by cofilin and myosin modifications that on the contrary are immediately dephosphorylated after treatment. This links the observed two-regime dissipation behaviour to a temporal cellular drug-response that is mediated by FAK, myosin, and cofilin.

5 Conclusion

Viscoelastic changes due to the treatment of MCF-7 with cytoskeleton-targeting drugs like CytoD and Y27632 were detected by QCM-D as dissipation shifts. The role of extracellular matrix proteins (like FN) in relation to QCM analysis and drug treatment was also investigated. By combining QCM-D and Optical/Confocal microscopy, the obtained QCM-D responses were validated and related to changes in cell morphology. The real-time and unique information gained from QCM-D revealed fine details in cytoskeleton modification that were not possible to completely address by only Optical/Confocal microscopy. Overall, these results indicate that the QCM-D allows a real-time monitoring of cytoskeletal alterations/dynamics and results appealing to study the mechanism of novel cytoskeleton-affecting drugs.

Acknowledgement

We gratefully acknowledge funding from the Apulia Regional Cluster project "SISTEMA" project code T7WGSJ3.

Conflict of interest

The authors declare no financial or commercial conflict of interest.

5 References

[1] Vergara, D., Simeone, P., del Boccio, P., Toto, C.*, et al.*, Comparative proteome profiling of breast tumor cell lines by gel electrophoresis and mass spectrometry reveals an epithelial mesenchymal transition associated protein signature. *Molecular bioSystems* 2013, *9*, 1127-1138.

[2] Vergara, D., Ferraro, M. M., Cascione, M., del Mercato, L. L.*, et al.*, Cytoskeletal Alterations and Biomechanical Properties of parkin-Mutant Human Primary Fibroblasts. *Cell biochemistry and biophysics* 2015, *71*, 1395-1404.

[3] Liao, J. K., Seto, M., Noma, K., Rho Kinase (ROCK) Inhibitors. *Journal of cardiovascular pharmacology* 2007, *50*, 17-24.

[4] Mehrotra, P., Biosensors and their applications – A review. *Journal of Oral Biology and Craniofacial Research* 2016, *6*, 153-159.

[5] Chen, J. Y., Penn, L. S., Xi, J., Quartz crystal microbalance: Sensing cell-substrate adhesion and beyond. *Biosens Bioelectron* 2018, *99*, 593-602.

[6] Kushiro, K., Lee, C.-H., Takai, M., Simultaneous characterization of protein-material and cell-protein interactions using dynamic QCM-D analysis on SAM surfaces. *Biomaterials Science* 2016, *4*, 989-997.

[7] Kandel, J., Lee, H.-S., Sobolewski, P., Tomczyk, N.*, et al.*, Chemically grafted fibronectin for use in QCM-D cell studies. *Biosensors & bioelectronics* 2014, *58*, 249-257.

[8] Chronaki, D., Stratiotis, D. I., Tsortos, A., Anastasiadou, E., Gizeli, E., Screening between normal and cancer human thyroid cells through comparative adhesion studies using the Quartz Crystal Microbalance. *Sensing and Bio-Sensing Research* 2016, *11*, 99-106.

[9] Elmlund, L., Käck, C., Aastrup, T., Nicholls, I. A., Study of the Interaction of Trastuzumab and SKOV3 Epithelial Cancer Cells Using a Quartz Crystal Microbalance Sensor. *Sensors (Basel, Switzerland)* 2015, *15*, 5884-5894.

[10] Fohlerová, Z., Skládal, P., Turánek, J., Adhesion of eukaryotic cell lines on the gold surface modified with extracellular matrix proteins monitored by the piezoelectric sensor. *Biosensors and Bioelectronics* 2007, *22*, 1896-1901.

[11] Fohlerová, Z., Turánek, J., Skládal, P., The cell adhesion and cytotoxicity effects of the derivate of vitamin E compared for two cell lines using a piezoelectric biosensor. *Sensors and Actuators B: Chemical* 2012, *174*, 153-157.

[12] Heitmann, V., Reiß, B., Wegener, J., The Quartz Crystal Microbalance in Cell Biology: Basics and Applications, in: Janshoff, A., Steinem, C. (Eds.), *Piezoelectric Sensors*, Springer Berlin Heidelberg, Berlin, Heidelberg 2007, pp. 303-338.

[13] Janshoff, A., Wegener, J., Sieber, M., Galla, H. J., Double-mode impedance analysis of epithelial cell monolayers cultured on shear wave resonators. *European Biophysics Journal* 1996, *25*, 93-103.

[14] Wegener, J., Janshoff, A., Galla, H. J., Cell adhesion monitoring using a quartz crystal microbalance: comparative analysis of different mammalian cell lines. *European Biophysics Journal* 1998, *28*, 26-37.

[15] Zhou, T., Marx, K. A., Warren, M., Schulze, H., Braunhut, S. J., The Quartz Crystal Microbalance as a Continuous Monitoring Tool for the Study of Endothelial Cell Surface Attachment and Growth. *Biotechnology Progress* 2000, *16*, 268-277.

[16] Matsuda, T., Kishida, A., Ebato, H., Okahata, Y., Novel instrumentation monitoring in situ platelet adhesivity with a quartz crystal microbalance. *ASAIO journal (American Society for Artificial Internal Organs : 1992)* 1992, *38*, M171-173.

[17] Redepenning, J., Schlesinger, T. K., Mechalke, E. J., Puleo, D. A., Bizios, R., Osteoblast attachment monitored with a quartz crystal microbalance. *Anal Chem* 1993, *65*, 3378-3381.

[18] Wegener, J., Janshoff, A., Galla, H. J., Cell adhesion monitoring using a quartz crystal microbalance: comparative analysis of different mammalian cell lines. *European biophysics journal : EBJ* 1999, *28*, 26-37.

[19] Fredriksson, C., Kihlman, S., Rodahl, M., Kasemo, B., The Piezoelectric Quartz Crystal Mass and Dissipation Sensor: A Means of Studying Cell Adhesion. *Langmuir* 1998, *14*, 248-251.

[20] Nimeri, G., Fredriksson, C., Elwing, H., Liu, L.*, et al.*, Neutrophil interaction with protein-coated surfaces studied by an extended quartz crystal microbalance technique. *Colloids and Surfaces B: Biointerfaces* 1998, *11*, 255-264.
[21] Otto, K., Elwing, H., Hermansson, M., Effect of ionic strength on initial interactions of Escherichia coli with surfaces, studied on-line by a novel quartz crystal microbalance technique. *Journal of bacteriology* 1999, *181*, 5210-5218.
[22] Reipa, V., Almeida, J., Cole, K. D., Long-term monitoring of biofilm growth and disinfection using a quartz crystal microbalance and reflectance measurements. *Journal of Microbiological Methods* 2006, *66*, 449-459.
[23] Alessandrini, A., Croce, M. A., Tiozzo, R., Facci, P., Monitoring cell-cycle-related viscoelasticity by a quartz crystal microbalance. *Applied Physics Letters* 2006, *88*, 083905.
[24] Galli Marxer, C., Collaud Coen, M., Greber, T., Greber, U. F., Schlapbach, L., Cell spreading on quartz crystal microbalance elicits positive frequency shifts indicative of viscosity changes. *Analytical and bioanalytical chemistry* 2003, *377*, 578-586.
[25] Li, F., Wang, J. H. C., Wang, Q.-M., Thickness shear mode acoustic wave sensors for characterizing the viscoelastic properties of cell monolayer. *Sensors and Actuators B: Chemical* 2008, *128*, 399-406.
[26] Marx, K. A., Zhou, T., Montrone, A., McIntosh, D., Braunhut, S. J., Quartz crystal microbalance biosensor study of endothelial cells and their extracellular matrix following cell removal: Evidence for transient cellular stress and viscoelastic changes during detachment and the elastic behavior of the pure matrix. *Analytical biochemistry* 2005, *343*, 23-34.
[27] Pax, M., Rieger, J., Eibl, R. H., Thielemann, C., Johannsmann, D., Measurements of fast fluctuations of viscoelastic properties with the quartz crystal microbalance. *The Analyst* 2005, *130*, 1474-1477.
[28] Voinova, M. V., Jonson, M., Kasemo, B., On dissipation of quartz crystal microbalance as a mechanical spectroscopy tool. *Spectroscopy* 2004, *18*.
[29] Rahlves, M., Roth, B., Reithmeier, E., Systematic errors on curved microstructures caused by aberrations in confocal surface metrology. *Optics express* 2015, *23*, 9640-9648.
[30] Tymchenko, N., Nileback, E., Voinova, M. V., Gold, J.*, et al.*, Reversible changes in cell morphology due to cytoskeletal rearrangements measured in real-time by QCM-D. *Biointerphases* 2012, *7*, 43.
[31] Kuddannaya, S., Chuah, Y. J., Lee, M. H. A., Menon, N. V.*, et al.*, Surface Chemical Modification of Poly(dimethylsiloxane) for the Enhanced Adhesion and Proliferation of Mesenchymal Stem Cells. *ACS Applied Materials & Interfaces* 2013, *5*, 9777-9784.
[32] Bianco, M., Aloisi, A., Arima, V., Capello, M.*, et al.*, Quartz crystal microbalance with dissipation (QCM-D) as tool to exploit antigen-antibody interactions in pancreatic ductal adenocarcinomadetection. *Biosens Bioelectron* 2013, *42*, 646-652.
[33] Bianco, M., Sonato, A., De Girolamo, A., Pascale, M.*, et al.*, An aptamer-based SPR-polarization platform for high sensitive OTA detection. *Sensors and Actuators B: Chemical* 2017, *241*, 314-320.
[34] Hsiao, S. T., Spencer, T., Boldock, L., Prosseda, S. D.*, et al.*, Endothelial repair in stented arteries is accelerated by inhibition of Rho-associated protein kinase. *Cardiovascular Research* 2016, *112*, 689-701.
[35] Kusakawa, Y., Yoshida, E., Hayakawa, T., Protein Adsorption to Titanium and Zirconia Using a Quartz Crystal Microbalance Method. *BioMed Research International* 2017, *2017*, 8.
[36] Hynes, R. O., Integrins: versatility, modulation, and signaling in cell adhesion. *Cell* 1992, *69*, 11-25.
[37] Singh, P., Carraher, C., Schwarzbauer, J. E., Assembly of fibronectin extracellular matrix. *Annual review of cell and developmental biology* 2010, *26*, 397-419.
[38] Afara, N., Omanovic, S., Asghari-Khiavi, M., Functionalization of a gold surface with fibronectin (FN) covalently bound to mixed alkanethiol self-assembled monolayers (SAMs): The influence of SAM composition on its physicochemical properties and FN surface secondary structure. *Thin Solid Films* 2012, *522*, 381-389.
[39] Tew, S. R., Hardingham, T. E., Regulation of SOX9 mRNA in Human Articular Chondrocytes Involving p38 MAPK Activation and mRNA Stabilization. *Journal of Biological Chemistry* 2006, *281*, 39471-39479.
[40] Silberberg, Y. R., Mieda, S., Amemiya, Y., Sato, T.*, et al.*, Evaluation of the actin cytoskeleton state using an antibody-functionalized nanoneedle and an AFM. *Biosensors and Bioelectronics* 2013, *40*, 3-9.

[41] Yanqun, T., Juhui, Q., Yiming, Z., Xiangdong, L*., et al.*, Effects of Type I Collagen and Fibronectin on Regulation of Breast Cancer Cell Biological and Biomechanical Characteristics. *Journal of Medical and Biological Engineering* 2014, *34*, 62-68.
[42] Leporatti, S., Vergara, D., Zacheo, A., Vergaro, V*., et al.*, Cytomechanical and topological investigation of MCF-7 cells by scanning force microscopy. *Nanotechnology* 2009, *20*, 055103.
[43] Wakatsuki, T., Schwab, B., Thompson, N. C., Elson, E. L., Effects of cytochalasin D and latrunculin B on mechanical properties of cells. *Journal of Cell Science* 2001, *114*, 1025.
[44] Maruta, H., PAKs, RAC/CDC42 (p21)-activated Kinases - Towards the Cure of Cancer and Other PAK-dependent Diseases. *Elsevier* 2013, 276.
[45] Shen, H., Zhou, T., Hu, J., A high-throughput QCM chip configuration for the study of living cells and cell-drug interactions. *Analytical and bioanalytical chemistry* 2017, *409*, 6463-6473.
[46] Staunton, J. R., Doss, B. L., Lindsay, S., Ros, R., Correlating confocal microscopy and atomic force indentation reveals metastatic cancer cells stiffen during invasion into collagen I matrices. *Scientific Reports* 2016, *6*, 19686.
[47] Eleanor, C. O., Lekhana, B., Amanda, E. B., Kristi, R. C*., et al.*, Analysis of microtubule growth dynamics arising from altered actin network structure and contractility in breast tumor cells. *Physical Biology* 2017, *14*, 026005.

Figure 1

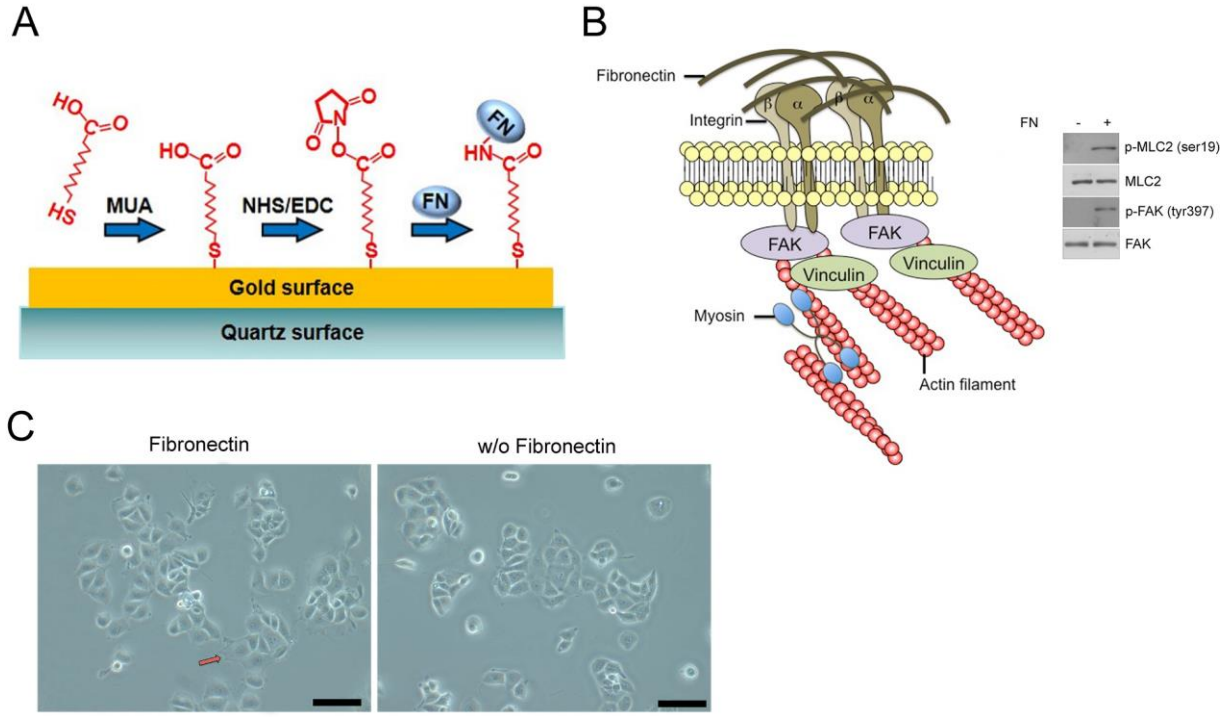

Figure 2

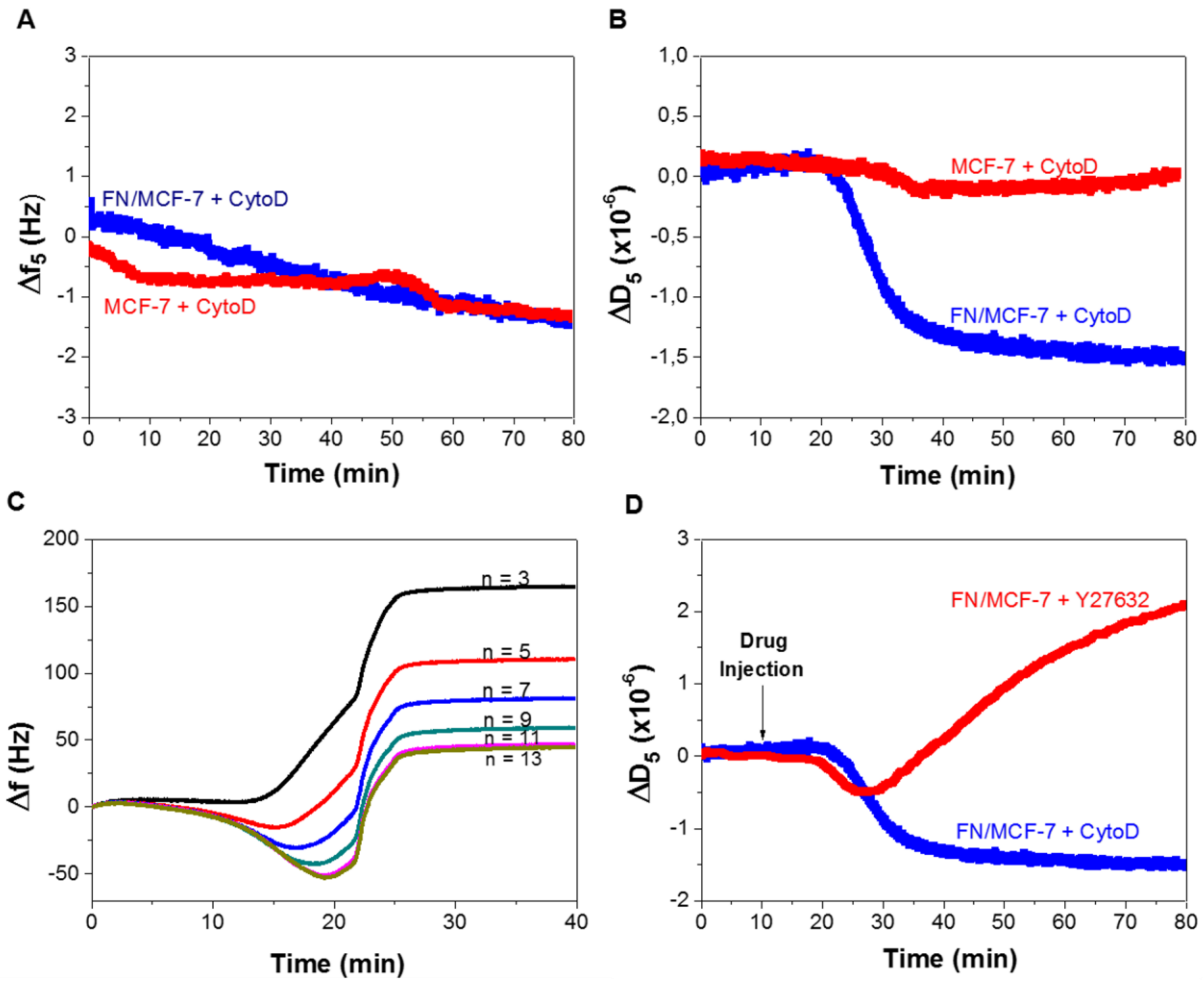

Figure 3

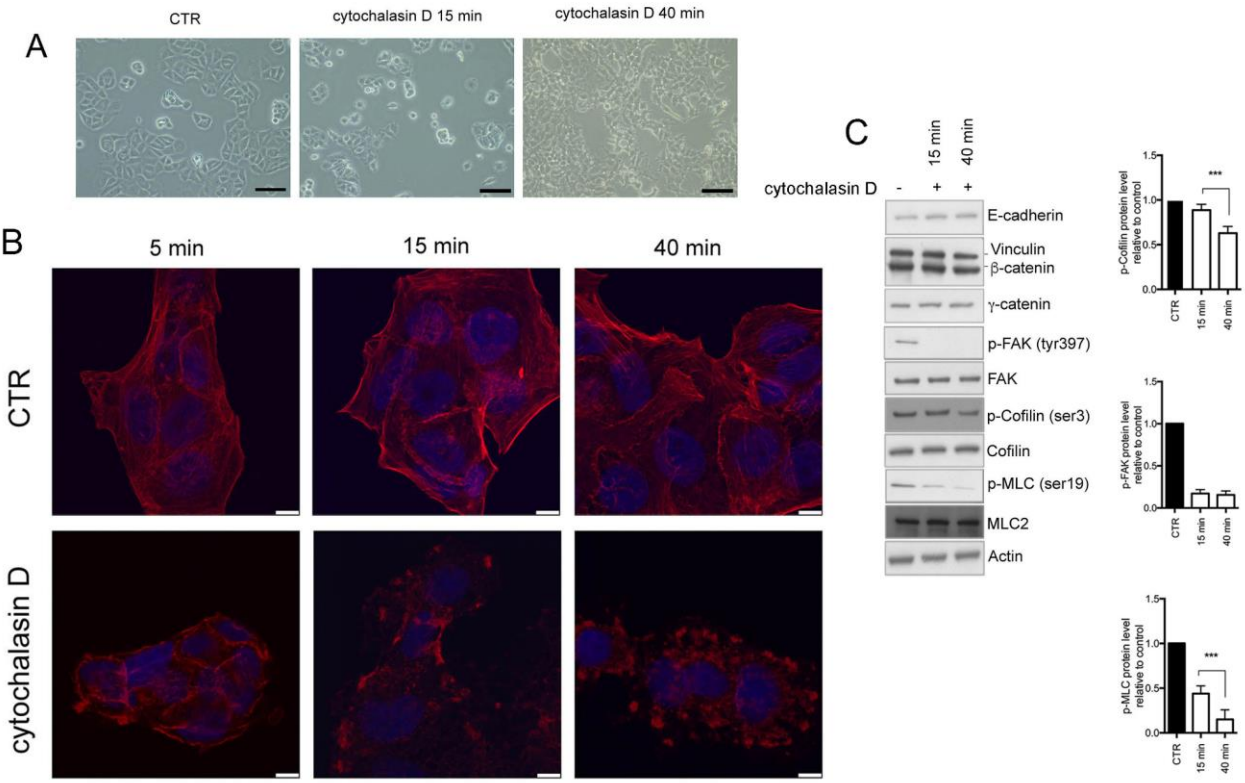

Figure 4

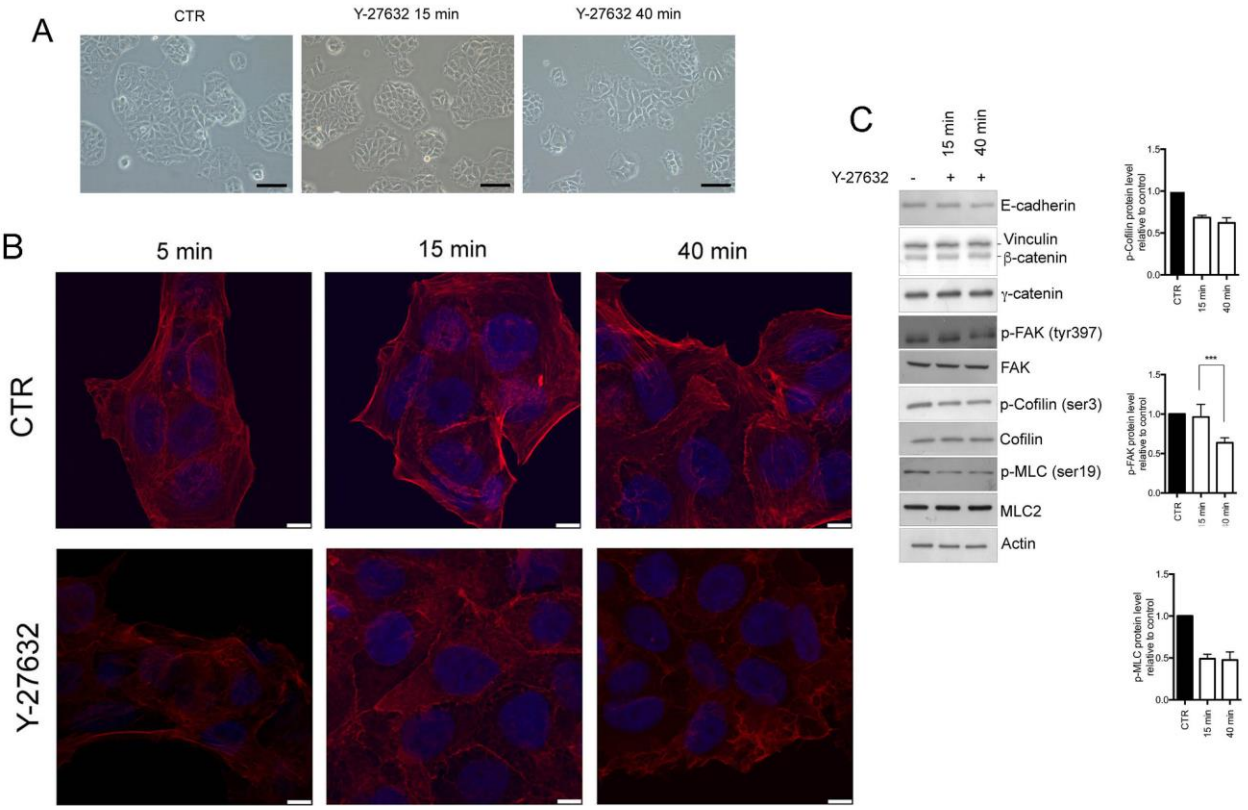

Supplementary Figure 1.

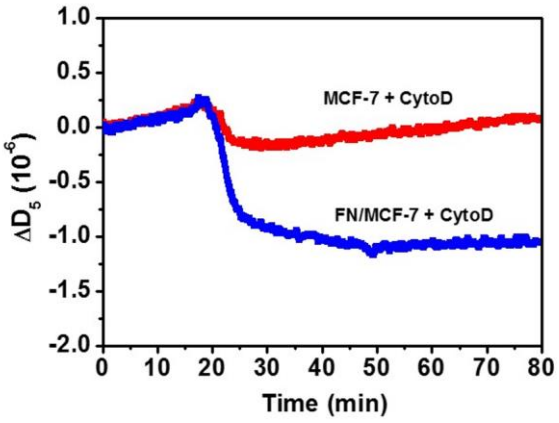

Supplementary Figure 2.

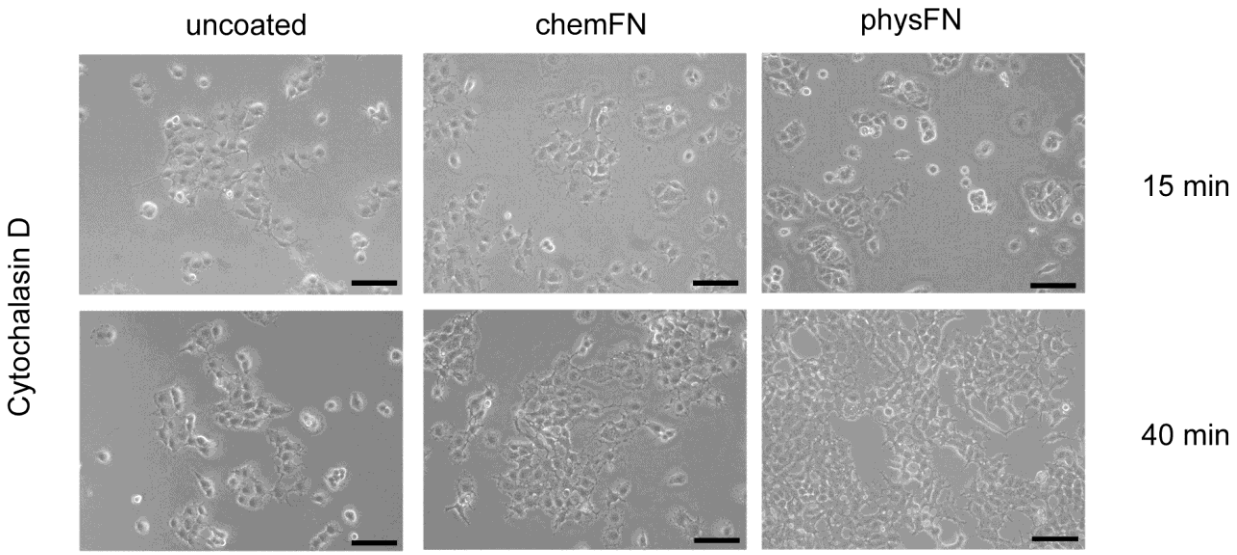

Figure legends

Figure 1. A) Scheme of the functionalization process by MUA/NHS/EDC of the QCM-D gold surface with FN. B) The actin-integrin-FN linkage is schematically depicted. FN promotes MCF-7 cell adhesion through FAK, and MLC. MCF-7 cells were seeded in dishes uncoated or coated with FN (10 μg/mL) and incubated for 40 min at 37 °C. Whole cell lysates were analysed by western blotting using the indicated antibodies. C) Representative bright-phase images of MCF-7 cells seeded on FN-coated (10 μg/mL) or uncoated dishes. Cytoplasmatic projections are evident on the FN-coated substrate (arrow). Scale bar 100 μm.

Figure 2. A) Resonance frequency changes and B) Dissipation Signal for gold quartz without and with FN coating covered by a MCF-7 layer (MCF-7 and FN/MCF-7) and treated with CytoD at 10 min. C) Stable L-15 baselines prior to the addition of drugs. Resonance frequency changes measured simultaneously at the six harmonics. D) Dissipation Signal monitoring in response to treatment (injection at 10 min) to Y27632 and CytoD of a QCM-D sensor coated by FN and MCF-7 (FN/MCF-7).

Figure 3. Morphological and molecular effects of actin inhibitors on MCF-7 cells. A) Representative bright-phase images of MCF-7 cells treated or not with 10 μM CytoD at two different time points. Images were obtained using an Olympus IX51 microscope, scale bar 100 μm (10x magnification). B) MCF-7 cells seeded without or with CytoD, stained with phalloidin (red) and counterstained with DAPI (blue) to visualize actin filaments and nuclei, respectively. Scale bar 75 μm. C) Western blot analyses of MCF-7 cells seeded on FN-coated dishes (10 μg/mL) in the presence or absence of 10 μM CytoD at two different time points with the indicated antibodies. Actin was used as loading control. Bar graphs show the densitometric measures of pCofilin/cofilin, pMLC/MLC, and pFAK/FAK ratio normalized to control cells. Data are expressed as mean ± SD of three independent experiments. Student's t-test was done using GraphPad Prism 6. *** $P < 0.001$.

Figure 4. Morphological and molecular effects of actin inhibitors on MCF-7 cells. A) Representative bright-phase images of MCF-7 cells treated or not with 10 μM Y-27632 at two different time points. Images were obtained using an Olympus IX51 microscope, scale bar 100 μm (10x magnification). B) MCF-7 cells seeded without or with Y-27632, stained with phalloidin (red) and counterstained with DAPI (blue) to visualize actin filaments and nuclei, respectively. Scale bar 75 μm. C) Western blot analyses of MCF-7 cells seeded on FN-coated dishes (10 μg/mL) in the presence or absence of 10 μM Y-27632 at two different time points with the indicated antibodies. Actin was used as loading control. Bar graphs show the densitometric measures of pCofilin/cofilin, pMLC/MLC, and pFAK/FAK ratio normalized to control cells. Data are expressed as mean ± SD of three independent experiments. Student's t-test was done using GraphPad Prism 6. *** $P < 0.001$.

Supplementary Figure 1. Dissipation Signal for gold quartz without and with FN coating covered by a MCF-7 layer deposited from a suspension of 33000 cells (MCF-7 and FN/MCF-7) and treated with CytoD at 10 min.

Supplementary Figure 2. Morphological effects of actin inhibitor CytoD on MCF-7 cells. Representative bright-phase images of MCF-7 cells seeded on FN-physically (physFN) or FN-chemically (chemFN) coated (10 μg/mL) or uncoated glass coverslips, and treated with CytoD at the concentration of 10 μM for 15 min and 40 min. Scale bar 100 μm.